

Enhancement of Photocatalytic Degradation of Polyvinyl Chloride Plastic with Fe₂O₃ Modified AgNbO₃ Photocatalyst under Visible-light Irradiation^①

CHANG Hai-Bo LIU Jun-Bo^②

DONG Zheng WANG Dan-Dan^a XIN Yu

JIANG Zhuo-Lin^a TANG Shan-Shan^a

(College of Resource and Environmental Science, Jilin Agricultural University, Changchun 130118, China)

ABSTRACT The solid-phase photocatalytic degradation of polyvinyl chloride (PVC) plastic with AgNbO₃/Fe₂O₃ is studied under visible-light irradiation. The PVC-(AgNbO₃/Fe₂O₃) samples are characterized by X-ray photoelectron spectroscopy (XPS), scanning electron microscope (SEM), gas chromatography (GC), and UV-vis diffusion reflectance spectra (UV-vis DRS). The photocatalytic properties of PVC-(AgNbO₃/Fe₂O₃) samples are systematically investigated. More amounts of generated CO₂, greater texture change and higher weight loss rate were exhibited in the system of PVC-(AgNbO₃/Fe₂O₃) than pure PVC film. The weight loss rate is ten times higher than that of pure PVC film, which reaches to 46.53% with optimum amount of 0.5 wt% Fe₂O₃. Active radicals generate primarily on the surface of Fe₂O₃ particles, which cause composite plastic decomposition on the PVC-(AgNbO₃/Fe₂O₃) interface and extend into polymer interior. The study provides a new promising way to degrade the plastic waste under visible-light.

Keywords: photocatalytic degradation, polyvinyl chloride, AgNbO₃/Fe₂O₃;

DOI: 10.14102/j.cnki.0254-5861.2011-3217

1 INTRODUCTION

PVC plastic materials have been extensively used in various fields. They are hardly biodegraded in natural environment owing to their chemical stability. They are usually incinerated with the production of quantities of dioxins. The high and diverse toxicities cause the most concerning environment and health problems^[1-3]. Actually, the field of PVC degradation has received increasing attention due to their long degradation cycle and incompleteness, which limits their application in industry and agriculture. Various methods have been made aiming at reducing the pollution. Photocatalytic technologies have been successfully utilized on developing environment friendly system by oxidizing organic pollutants. Many researchers have reported that PVC and polyethylene plastic can be degraded over photocatalysts TiO₂ in the open air to improve the environment^[4, 5]. However, a large intrinsic band gap of

TiO₂ is 3.2 eV allowing only a small portion of solar spectrum in UV light region to be absorbed^[6, 7].

Silver niobate (AgNbO₃) with perovskite structure is a multifunctional semiconductor material, which has been applied in microwave communication, microelectronics technology and photocatalysis^[8-10]. The band gap of AgNbO₃ is 2.8 eV, and this higher-energy valence band derives from the filled Ag 4d orbitals, making the valence bands at more negative levels than the O 2p orbitals and maintain a conduction band level high enough to reduce water and possess the ability to form H₂ and O₂^[11]. Many effective methods have been carried out to modify the AgNbO₃ to enhance their photocatalytic activity. Yang et al. indicated that when Ag was doped on the surface of AgNbO₃, their photocatalytic activity can be remarkably promoted in comparison with that of pure AgNbO₃^[12]. Sun et al. studied NiO nanoparticle formed on the surface of AgNbO₃, which improved the optical absorption and photocatalytic activity in

Received 14 April 2021; accepted 12 July 2021

① Supported by Science and Technology Department of Jilin Province (20200101018JC, 20190303086SF and 20200201011JC)

② Corresponding author. E-mail: liujb@mail.ccut.edu.cn

the visible region^[13]. Fe₂O₃ with narrow band gap (2.2 eV) is also a semiconductor photocatalytic material. Researchers found that the Fe₂O₃-doped TiO₂ effectively enhanced the photocatalytic property^[14, 15]. Lin reported that hematite and maghemite were used to activate H₂O₂ to produce hydroxyl radicals (\cdot OH) decomposing organic pollutants to water, carbon dioxide and inorganic salts^[16]. While, the photocatalytic properties of AgNbO₃ are mainly focused on the degradation of dye and water splitting^[17-19]. The Fe₂O₃ modified AgNbO₃ photocatalyst used in the PVC film is rarely reported.

In this article, a new kind of photocatalytic decomposition PVC-(AgNbO₃/Fe₂O₃) was prepared and their photocatalytic degradation characters were investigated under visible-light irradiation. The degradation product was detected and the possible mechanism was discussed.

2 EXPERIMENTAL

2.1 Materials

PVC, tetrahydrofuran (THF), ferric sulfate [Fe₂(SO₄)₃·9H₂O] and cetylpyridinium chloride were afforded by Sinopharm Chemical Reagent Co., Ltd. The average molecular weight of PVC was about 100,000. Deionized water was obtained from central of prepared water.

2.2 Preparation of AgNbO₃ and AgNbO₃/Fe₂O₃ photocatalysts

In a typical procedure, 14 mL NaOH (0.6 mol·L⁻¹) solution was slowly dropped into 3.75~26.25 mL Fe₂(SO₄)₃ (0.1 mol·L⁻¹) solution under vigorous stirring. And then 0.20 g cetylpyridinium chloride and 0.60 g AgNbO₃ were added to the above solution (The synthetic procedure of original AgNbO₃ were described in our previous paper^[20, 21]). The mixtures were stirred continuously for 4 h. The final mixture was putted into a Teflon-lined stainless-steel autoclave and heated at 180 °C for 2 h under autogenous pressure. The collected crystals were centrifuged for several times with distilled water, and dried at 60 °C. The brick red AgNbO₃/Fe₂O₃ photocatalyst was obtained containing 0.1 wt%, 0.3 wt%, 0.5 wt% and 0.7wt% Fe₂O₃, respectively.

2.3 Preparation of PVC-AgNbO₃ and

PVC-(AgNbO₃/Fe₂O₃) composite films

1.0 g PVC particles were dissolved in 20 mL THF under stirring for 4 h and ultrasonic vibration for 1 h. And then 0.03 g AgNbO₃ or AgNbO₃/Fe₂O₃ was added into PVC solution with the ratio of AgNbO₃ or AgNbO₃/Fe₂O₃ to PVC 3 wt%.

The above solution was sequentially stirred for 1 h. The films were achieved on the spin-coater machine. The viscous solution was spread on a tile surface, which was cleaned in ultrasonic deionized water and acetone bath to remove impurities. And then the films were kept in dark place for 72 h at room temperature. The pure PVC film was prepared by a similar procedure only without adding AgNbO₃ or AgNbO₃/Fe₂O₃.

2.4 Photodegradation and characterization of the PVC-AgNbO₃ and PVC-(AgNbO₃/Fe₂O₃) composite films

All films were washed several times by deionized water in order to remove the traces of THF solvent. Every piece of composite film was cut into the dimensions with 4cm × 4cm. All the films were measured to be 20 μm by a micrometer. The photocatalytic degradation was performed with 350 W xenon lamp as a visible-light source, which was positioned 15 cm away from the films in the ambient air. The UV-cutoff-filter was equipped providing visible light with ≥400 nm. The average light intensity striking the surface of the composite films was about 80 mW·cm⁻².

The computation formula of the weight loss was as follows:

$$C = (m_0 - m_t) / m_0 \times 100\%$$

Among them, C (%) was the weight loss of PVC composite films, and m_0 (g) and m_t (g) were the quality of PVC composite films before and after photocatalytic degradation, respectively.

The data of particles and films were obtained by the powder X-ray diffraction (XRD, Rigaku D/Max 2500 V/PC, Tokyo, Japan) using CuK α radiation ($\lambda = 1.5418 \text{ \AA}$) in the 2θ range of 20°~80°. Elemental composition and surface chemistry of samples were collected by X-ray photoelectron spectra (XPS, Tokyo, Japan) with a PHI 1600 spectroscope and MgK α X-ray source for excitation. The concentration of generated CO₂ in the process of degradation was detected by GC equipped with thermal conductivity detector (TCD) using GDX-43 steel column. The surface morphologies of composite films were performed by a scanning electronic microscope (SEM, JEOL JSM-7001F). UV-vis diffuse reflectance spectra were recorded on a UV-vis spectrophotometer (DRS, Hitachi U-4100 Japan) in order to obtain the absorption spectra of films. The 350 W xenon lampas (BL-GHX-V, Shanghai Bilang Instrument Co. Ltd.) as a visible-light source was used.

3 RESULTS AND DISCUSSION

3.1 XRD analysis of AgNbO₃/Fe₂O₃ samples

The XRD patterns of AgNbO₃/Fe₂O₃ are shown in Fig. 1. The peak shape of AgNbO₃ is sharp with high intensity, indicating its wonderful crystallinity, which is completely consistent with the standard spectrogram (JCPDS No. 52-0405) (Fig. 1a). The Fe₂O₃ nanoparticles show sharp diffraction peak, high crystallinity and high purity as shown

in Fig. 1b (JCPDS No. 33-0664). According to the following degradation experiment, the AgNbO₃/Fe₂O₃ samples prepared with 0.5 wt% Fe₂O₃ are chosen for characterization. Fig. 1c illustrates that Fe₂O₃ nanoparticles are successfully loaded on the surface of AgNbO₃. The diffraction peaks of Fe₂O₃ locate at 2θ are 33.1°, 35.6°, 54.1° and 63.9° corresponding to crystal indices of (104), (110), (116) and (300), respectively, which are marked with * in Fig. 1c. The other diffraction peaks are assigned to AgNbO₃.

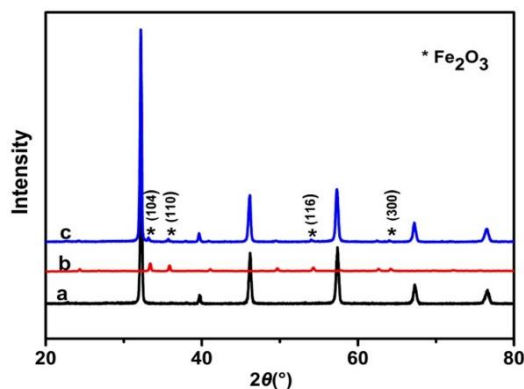


Fig. 1. Patterns of AgNbO₃ (a), Fe₂O₃ (b) and AgNbO₃/Fe₂O₃ (c)

3.2 XPS analysis of PVC-(AgNbO₃/Fe₂O₃) samples

To gain an insight into the existence states of AgNbO₃/Fe₂O₃ in the film, the XPS spectra are conducted and displayed in Fig. 2. The survey spectrum indicates that the composite film includes Ag, Nb, Fe, O, C and Cl elements. The peak of C 1s at 280 eV owns to adventitious hydrocarbon from XPS instrument. Moreover, the peak at the binding energy of 199.6 eV attributes to C–Cl chemical composite of composite film (Fig. 2a). The XPS spectrum of Ag is shown in Fig. 2b. Two peaks at 373.9 and 367.8 eV are assigned to Ag 3d_{3/2} and 3d_{5/2}, respectively. The peaks at 367.8 and 373.9 eV are associated with the binding energies of Ag⁺ inside AgNbO₃, as reported in the earlier literatures^[22]. Moreover, the XPS spectrum of Fe exhibits two peaks at

711.3 and 725.1 eV related to Fe 2p_{3/2} and 2p_{1/2}, respectively (Fig. 2c). The result is consistent with the previous report for pure hematite power and films^[23]. The energy difference is 14 eV between Fe 2p_{3/2} and Fe 2p_{1/2} peaks, which is characteristic of Fe³⁺ state, demonstrating the formation of α -Fe₂O₃ by experimental methodology that Souza et al. have reported^[24]. Meanwhile, it is clearly seen in the spectrum that the Fe³⁺ satellite peak is centered at 718 eV, above the Fe 2p_{3/2} peak. The doublet spin orbits of Fe 2p_{3/2} and Fe 2p_{1/2} indicate successful loading Fe₂O₃ on the surface of AgNbO₃. In Fig. 2d, there is one component of O 1s, corresponding to 530.3 eV. The intense peak corresponds to the oxygen bonded as α -Fe₂O₃.

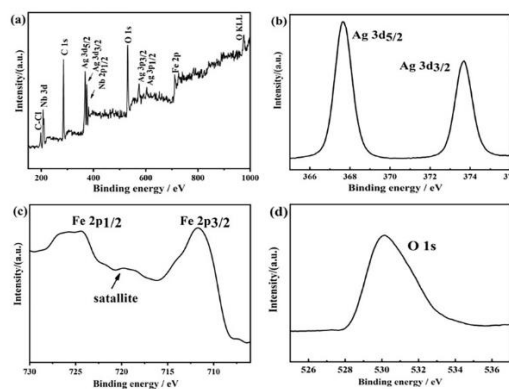


Fig. 2. Survey scan XPS spectra of PVC-(AgNbO₃/Fe₂O₃) samples (a) and details of the Ag 3d (b), Fe 2p (c) and O 1s (d)

3. 3 Photocatalytic degradation of PVC-AgNbO₃ and PVC-(AgNbO₃/Fe₂O₃) samples

In order to reveal the photocatalytic degradation behavior and mechanism of different PVC films, the photodegradation reaction is carried out under xenon lamp at room temperature. The photocatalytic activities of these films are assessed directly by weight loss rate in Fig. 3. After irradiation for 120 min, the weight loss rate for pure PVC film is only 4.09% with pretty low photocatalytic activity, and is less than 18% for PVC-(AgNbO₃). While, the weight loss rates of PVC-(AgNbO₃/Fe₂O₃) with different amounts of Fe₂O₃ doping are estimated to be from 20.36% to 46.53%. They are remarkably increased with raising the amount of Fe₂O₃. The highest value of weight loss rate is 46.53% with optimum amount of

0.5 wt% Fe₂O₃, displaying the Fe₂O₃ particles play an important role in promoting the photocatalytic degradation of PVC films. The result illustrates all the active species can be introduced to polymer and exhibit an optimal surface concentration at submonolayer coverage, when both AgNbO₃ and Fe₂O₃ particles enter into the surface of PVC polymer. Meanwhile, the weight loss rate decreases to 43.81% at the amount of 0.7 wt% Fe₂O₃ due to the excess Fe₂O₃ loaded on the active centre of AgNbO₃, thus reducing the reactive group in the solution and decreasing the photocatalytic performance. The above weight loss data reveal that the photocatalytic reaction of PVC-(AgNbO₃/Fe₂O₃) occurs and might produce a mass of volatile products, such as carbon dioxide, ethene, propane and so on.

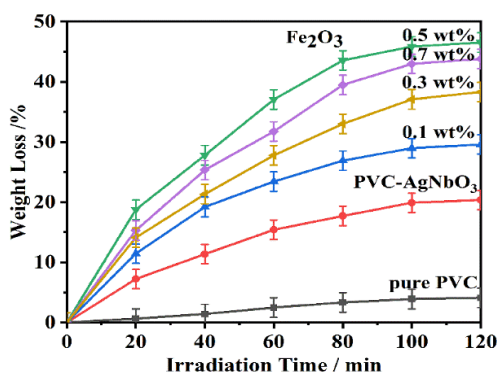


Fig. 3. Weight loss of pure PVC, PVC-AgNbO₃ and PVC-(AgNbO₃/Fe₂O₃) samples with visible-light irradiation

The formation of CO₂ in weight loss of films is evaluated by GC and shown in Fig. 4. After visible-light irradiation for 100 min, the total amount of CO₂ produced during photodegradation process accounts for 90% and 95% of the weight loss of PVC-AgNbO₃ and PVC-(AgNbO₃/Fe₂O₃), respectively. Pure PVC was only slightly decomposed. CO₂ is the major product of the photocatalytic degradation in the

degradation process of PVC plastic and it is environmentally friendly. There are two types of degradation in the whole process, which are photolytic degradation and photocatalytic degradation for PVC-AgNbO₃ and PVC-(AgNbO₃/Fe₂O₃) samples. However, CO₂ was produced only from photolytic degradation for pure PVC film.

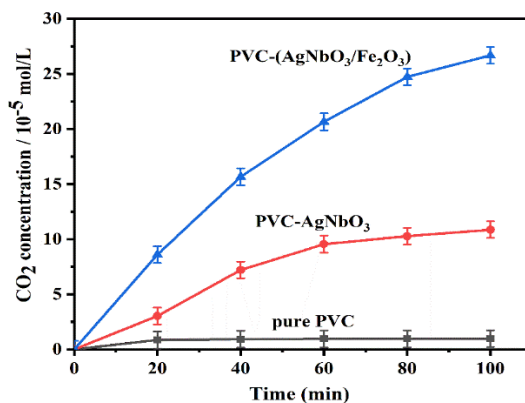


Fig. 4. Concentration of CO₂ for pure PVC, PVC-AgNbO₃ and PVC-(AgNbO₃/Fe₂O₃) samples with visible-light irradiation

Fig. 5 shows the texture of different samples before and after visible-light irradiation. As shown in Fig. 5a, the surface of pure PVC film is smooth. However, some irregular particles with heterogeneous size are stacked closely on surfaces of PVC-AgNbO₃ and PVC-(AgNbO₃/Fe₂O₃), respectively (Fig. 5c, 5e). PVC-(AgNbO₃/Fe₂O₃) with 0.5% Fe₂O₃ is elected as an example. After irradiation for 120 min, samples noticeably changed and cavities formed with holes. There are some holes with 1~3 μm on surface of pure PVC film (Fig. 5d). In contrast to pure PVC film, the dense

network structures with the sizes of 5~10 and 20~30 μm form on the surface of PVC-AgNbO₃ and PVC-(AgNbO₃/Fe₂O₃), respectively (Fig. 5f, 5e), which illustrate that the photodegradation of PVC primarily happens on film surface. The cavities are formed around AgNbO₃ and AgNbO₃/Fe₂O₃ particles because photocatalytic reaction firstly occurs at the interface among PVC, AgNbO₃ and AgNbO₃/Fe₂O₃. The photocatalytic reaction led to band scission of PVC-AgNbO₃ or PVC-(AgNbO₃/Fe₂O₃).

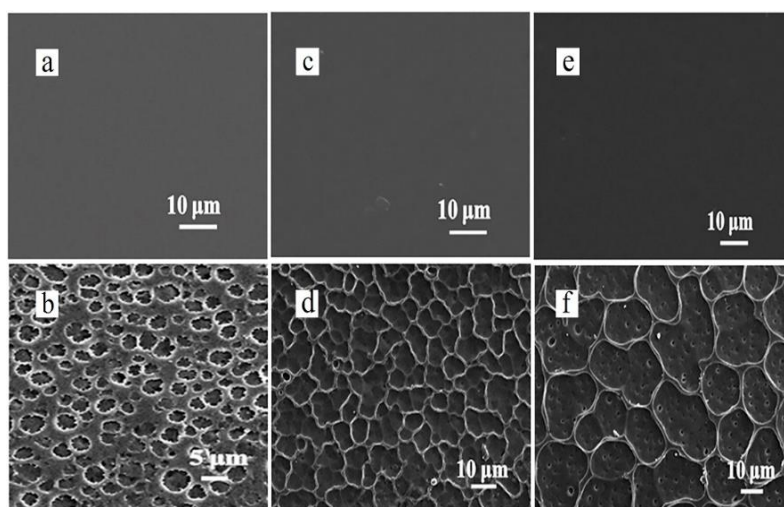


Fig. 5. SEM images of different films before and after irradiation for 120 min. Pure PVC films before (a) and after (b) irradiation, PVC-AgNbO₃ before (c) and after (d) irradiation, PVC-(AgNbO₃/Fe₂O₃) before (e) and after (f) irradiation

The FT-IR spectra of PVC-(AgNbO₃/Fe₂O₃) films before and after visible-light irradiation for 120 min are shown in Fig. 6. The spectra of the composite films show the characteristic absorption of long alkyl chain in the region of 2927~2858 cm^{-1} . The intense sharp peak at about 908 cm^{-1}

results from C-Cl stretching vibration of PVC. After irradiation for 120 min, a new absorption peak present at 1724 cm^{-1} would be assigned to C=O stretching vibrations^[25]. Visible-light irradiation constantly induces the composites film to dehydrochlorination and form double bonds.

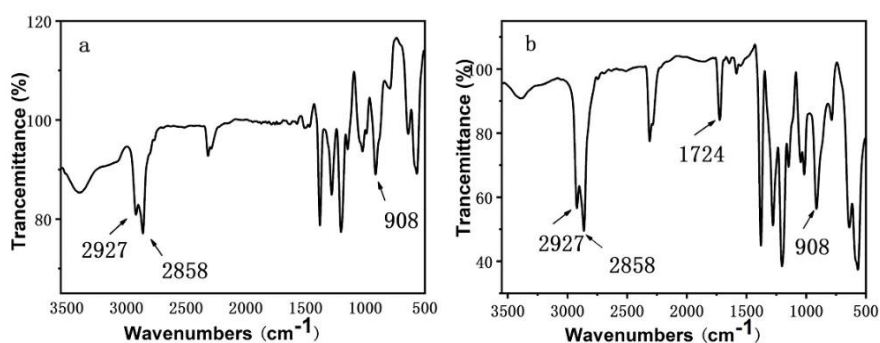


Fig. 6. FT-IR spectra of PVC-(AgNbO₃/Fe₂O₃) films before (a) and after visible-light irradiation (b)

3. 4 Effect of the addition of the amount of Fe₂O₃

Photodegradation efficiency of PVC composite films is related to the amount of Fe₂O₃. The weight loss rates are

strongly dependent on the mass ratio of Fe₂O₃ from 0.1 to 0.7 wt%. Dhananjeyan et al reported that PE film was degraded via Fe₂O₃ doped TiO₂ under UV irradiation. The

photoresponse could be enhanced by doping Fe₂O₃ into TiO₂ attributed to the separation of photogenerated charge. The result reveals that photodegradation efficiency can be promoted by increasing the amount of Fe₂O₃^[26]. The surface morphologies of PVC-(AgNbO₃/Fe₂O₃) samples after visible-light irradiation for 120 min are shown in Fig. 7. All the samples are obviously decomposed. There are some cavities around the AgNbO₃/Fe₂O₃ particles in composite films. The cavity sizes are from 10 to 30 μ m with changing the amount of Fe₂O₃ from 0.1 to 0.5 wt% (Fig. 7a~7c). SEM images illustrate that the degradation of films starts from interface

and leads to the formation of cavities around the photocatalyst. While, the cavity sizes diminish when the amount of Fe₂O₃ increases to 0.7 wt% (Fig. 7d). The result corresponds with previous studies in section 3. 3 (Fig. 3), which demonstrates the Fe₂O₃ coverage on the surface of AgNbO₃ would significantly affect the photocatalytic activity. The Fe₂O₃ could improve the efficiency of charge separation and inhibit the recombination of electrons and holes. But excess Fe₂O₃ decreases the photodegradation efficiency of PVC composite films.

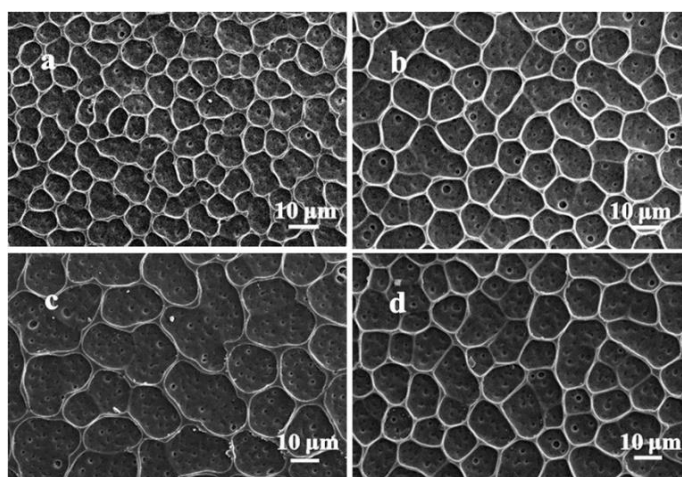


Fig. 7. SEM images of variations amount of Fe₂O₃ in PVC-(AgNbO₃/Fe₂O₃) samples after visible-light irradiation for 120 min. (a) 0.1 wt%, (b) 0.3 wt%, (c) 0.5 wt%, (d) 0.7 wt%

3. 5 Spectroscopic characterization

The optical properties of different photocatalysts are evaluated by UV-vis absorption spectroscopy. As displayed in Fig. 8a, two samples with AgNbO₃ present broad and obvious absorption in visible light region after modification. The absorption range of AgNbO₃/Fe₂O₃ is remarkably broader than that of AgNbO₃ sample. The red shift of absorption threshold is up to around 580 nm attributed to the effect of Fe₂O₃. In the diffuse reflection mode, a part of incident light is absorbed by sample, which reduces the intensity of reflection light. Therefore, the baseline absorption is enhanced^[27]. In addition, the optical band gap

E_g of a semiconductor is deduced using the following equation: $(Ah\nu)^2 = h\nu - E_g$, where, A , h , ν and E_g represent the absorption coefficient, the Planck's constant, the incident photon frequency and the band gap, respectively. The band gap values are determined by the curves extrapolations, as shown in Fig. 8b. The E_g value of AgNbO₃ sample in this study is 2.9 eV. The direct transition of AgNbO₃/Fe₂O₃ sample is at 2.5 eV corresponding to the $O^{2-} 2p \rightarrow Fe^{3+} 3d$ charge transfer^[28, 29]. These results might be conducive to improve the photocatalytic activity of the AgNbO₃/Fe₂O₃ sample.

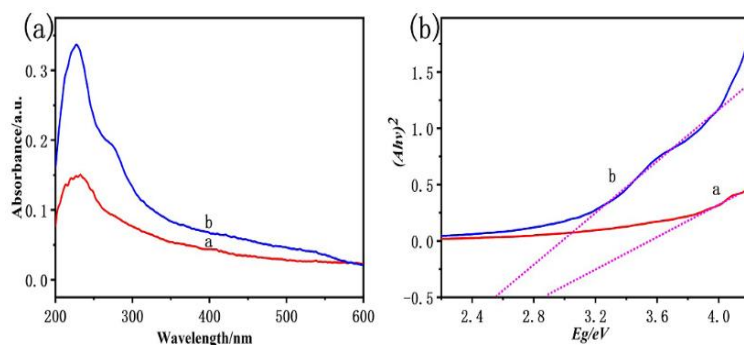


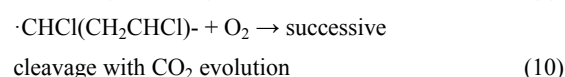
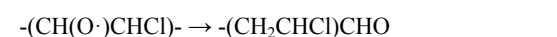
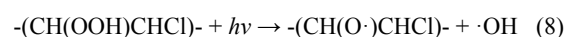
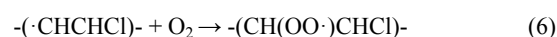
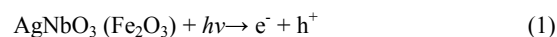
Fig. 8. UV-vis absorption spectra of different samples: (a): AgNbO₃, (b): AgNbO₃/Fe₂O₃ (containing 0.5% Fe₂O₃)

3.6 Photocatalytic degradation mechanism of PVC-(AgNbO₃/Fe₂O₃) samples

The photocatalytic degradation of pure PVC film has been extensively researched. Several researchers have reported that the photodegradation process of pure PVC film included two aspects^[30]. One step is the chain dehydrochlorination reaction, which could happen in both aerobic and anaerobic conditions. The C-Cl removes chlorine free radicals to form a double bond in the main chain. The PVC chain oxidation is the second step. The hydrogen atoms on the neighboring PVC polymer chains are attacked by peroxy radicals to form hydrogen peroxide. The successive reactions are carried out in the polymer chain cleavage when the carbon-centered radicals are introduced in the polymer chains^[31].

Band gap energies of AgNbO₃ and Fe₂O₃ particles are 2.86 and 2.21 eV, respectively. Their light absorption threshold wavelengths are calculated as 442 and 564 nm by formula $\lambda = 1240/E_g$. The electrons are excited from the valence bands of AgNbO₃ and Fe₂O₃ to their conduction bands, and holes are left in the valence band, respectively. The photoexcited electrons migrate from the conduction band of AgNbO₃ (CB = -0.81 eV) to the conduction band of Fe₂O₃ (CB = 0.1 eV) due to the slightly lower level of conduction band of Fe₂O₃, enhancing the charge separation efficiency. The level of the conduction band of Fe₂O₃ would not reduce the O₂ to $\cdot\text{O}_2^-$ (O₂/ $\cdot\text{O}_2^-$ = -0.33 eV). Therefore, H₂O₂ could be generated by direct reduction of O₂ by e⁻^[32, 33]. The induced electrons in the CB of Fe₂O₃ are captured by H₂O₂ to generate $\cdot\text{OH}$ radicals, which are important active radicals for the degradation of PVC films. Meanwhile, the holes in the valence band of Fe₂O₃ (VB = 2.31 eV) transfer to the surface of AgNbO₃ (VB = 2.05 eV). The transferred holes will cause the oxidation H₂O or OH⁻ to produce highly active $\cdot\text{OH}$ radicals with higher redox power. Therefore, the electrons in CB and the

holes with strong oxidation potential in the VB are separated effectively under visible-light irradiation. Subsequently, the PVC films could be oxidized by $\cdot\text{OH}$ and generated a series of intermediates. The intermediates are oxidized to CO₂ and volatile substances by the aid of reactive oxygen species as Eqs. (1~10)^[34, 35].



In addition, some photo electrons originating from Fe₂O₃ are immediately picked up by Fe³⁺, which causes the oxidation of Fe²⁺ to Fe³⁺. However, Fe²⁺ is not stable and is rapidly oxidized to Fe³⁺ by dissolved oxygen, thus leading to inner recycles^[36]. The photocatalytic reaction process of composite film under visible-light irradiation is shown in Fig. 9. Appropriate amount of Fe₂O₃ could improve the efficiency of charge separation and inhibit the recombination of electrons and holes. In the meantime, Fe³⁺ is reduced to Fe²⁺ during excitation. Fe²⁺ might be reacted with H₂O₂ to produce $\cdot\text{OH}$ and separated from surface of oxide to generate a vacancy^[37]. Besides, excessive amount of Fe₂O₃ would cause the reduction efficiency of electron and holes separation.

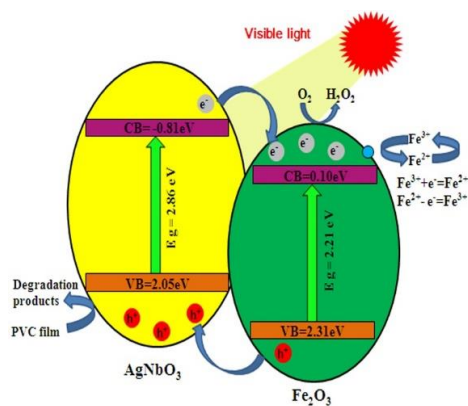


Fig. 9. Proposed schematic diagram of electron-hole separation of AgNbO₃/Fe₂O₃ particles under visible-light irradiation

4 CONCLUSION

In summary, PVC-(AgNbO₃/Fe₂O₃) samples are successfully prepared and the photocatalytic degradation process has been investigated under visible-light irradiation. Compared with pure PVC film, the degradation process of PVC-

(AgNbO₃/Fe₂O₃) could be controlled by changing the amount of Fe₂O₃ particles. The weight loss rate of PVC-(AgNbO₃/Fe₂O₃) is two times higher than that of PVC-AgNbO₃ and ten times higher than that of pure PVC film, respectively. The PVC-(AgNbO₃/Fe₂O₃) would become a potential photodegradable polymer material.

REFERENCES

- (1) Allahbakhsh, A. PVC/rice straw/SDBS-modified graphene oxide sustainable nanocomposites: melt mixing process and electrical insulation characteristics. *Compos. Part. A. Appl. Sci. Manuf.* **2020**, 134, 105902–1059010.
- (2) Harper, B. J.; Clendaniel, A.; Sinche, F.; Way, D.; Hughes, M. Impacts of chemical modification on the toxicity of diverse nanocellulose materials to developing zebrafish. *Cellulose* **2016**, 23, 1763–1775.
- (3) Zhou, G. Y.; Zhao, X. D.; Dong, B. B.; Liu, C. T. Improvement of the dispersity of micronano particles for PP/PVC composites using gas-assisted dispersion in a controlled foaming process. *Polym. Eng. Sci.* **2020**, 60, 524–534.
- (4) Wang, M. G.; Han, J.; Hu, Y. M.; Guo, R.; Yin, Y. D. Carbon-incorporated NiO/TiO₂ mesoporous shells with p-n heterojunctions for efficient visible light photocatalysis. *ACS. Appl. Mater. Interfaces* **2016**, 8, 29511–29521.
- (5) Teramura, K.; Tsunehiro, A.; Funabiki, T. Photoassisted selective catalytic reduction of NO with ammonia in the presence of oxygen over TiO₂. *Langmuir*. **2017**, 19, 1209–1214.
- (6) Abd El-Lateef, Hany M.; Mohamed, I. M. A.; Zhu, J. H.; Khalaf, M. M. An efficient synthesis of electrospun TiO₂-nanofibers/Schiff base phenylalanine composite and its inhibition behavior for C-steel corrosion in acidic chloride environments. *J. Taiwan. Inst. Chem. E* **2020**, 112, 306–321.
- (7) Wei, S. Y.; Chen, Y. B.; Hu, X. Y.; Wang, C. H.; Huang, X. J.; Liu, D. Q.; Zhang, Y. F. Monovalent/divalent salts separation via thin film nanocomposite nanofiltration membrane containing aminated TiO₂ nanoparticles. *J. Taiwan Inst. Chem. E.* **2020**, 112, 169–179.
- (8) Yang, L. F.; Liu, J. B.; Chang, H. B.; Tang, S. S. Enhancing the visible-light-induced photocatalytic activity of AgNbO₃ by loading Ag@AgCl nanoparticles. *RSC. Adv.* **2015**, 5, 59970–59975.
- (9) Gao, J.; Liu, Q.; Dong, J. F.; Wang, X. P.; Li, J. F. Local structure heterogeneity in Sm-doped AgNbO₃ for improved energy-storage performance. *ACS. Appl. Mater. Interfaces* **2020**, 12, 6097–6107.
- (10) Li, G.; Yan, S.; Wang, Z.; Wang, X.; Li, Z.; Zou, Z. Synthesis and visible light photocatalytic property of polyhedron-shaped AgNbO₃. *Dalton. T.* **2009**, 13, 2423–2427.
- (11) Li, G. Q.; Bai, Y.; Liu, X. Y.; Zhang, W. F. Surface photoelectric properties of AgNbO₃ photo-catalyst. *J. Phys. D.* **2009**, 42, 1–4.
- (12) Yang, L.; Shen, Q. Y.; Yu, Q. N.; Zhang, F.; Li, G. Q.; Zhang, W. F. Photoinduced *in-situ* growth of Ag nanoparticles on AgNbO₃. *J. Phys. Chem. C* **2016**, 120, 28712–28716.
- (13) Shu, H.; Xie, J.; Xu, H. Structural characterization and photocatalytic activity of NiO/AgNbO₃. *J. Alloys. Compounds* **2010**, 496, 633–637.

- (14) Lv, X. X.; Deng, J. J.; Sun, X. H. Cumulative effect of Fe_2O_3 on TiO_2 nanotubes via atomic layer deposition with enhanced lithium ion storage performance. *Appl. Surf. Sci.* **2016**, 369, 314–319.
- (15) Pang, Y. L.; Lim, S.; Tong, H. C.; Chong, W. T. Synthesis, characteristics and sonocatalytic activities of calcined $\gamma\text{-Fe}_2\text{O}_3$ and TiO_2 nanotubes/ $\gamma\text{-Fe}_2\text{O}_3$ magnetic catalysts in the degradation of Orange G. *Ultrason Sonochem.* **2016**, 29, 317–327.
- (16) Lin, Y. F.; Chang, C. Y. Design of composite maghemite/hematite/carbon aerogel nanostructures with high performance for organic dye removal. *Sep. Purif. Technol.* **2015**, 149, 74–81.
- (17) Wang, C.; Yan, J.; Wu, X. Y.; Song, Y. H.; Cai, G. B. Synthesis and characterization of $\text{AgBr}/\text{AgNbO}_3$ composite with enhanced visible-light photocatalytic activity. *Appl. Surf. Sci.* **2013**, 273, 159–166.
- (18) Kato, H.; Kobayashi, H.; Kudo, A. Role of Ag^+ in the band structures and photocatalytic properties of AgMO_3 (M: Ta and Nb) with the perovskite structure. *J. Phys. Chem. C* **2002**, 106, 12441–12447.
- (19) Yashima, M.; Matsuyama, S.; Sano, R.; Itoh, M.; Tsuda, K.; Fu, D. S. Structure of ferroelectric silver niobate AgNbO_3 . *Chem. Mater.* **2011**, 23, 1643–1645.
- (20) Chang, H. B.; Shang, M. Y.; Zhang, C. Y.; Yuan, H. M.; Feng, S. H. Hydrothermal syntheses and structural phase transitions of AgNbO_3 . *J. Am. Ceram. Soc.* **2012**, 95, 3673–3677.
- (21) Wang, D. D.; Liu, L. B.; Chang, H. B.; Tang, S. S. $\text{AgNbO}_3/\text{PVC}$ film with highly photocatalytic activity under visible light. *Chem. J. Chin. U.* **2014**, 9, 1975–1981.
- (22) Muduli, R.; Pattanayak, R.; Raut, S. Dielectric ferroelectric and Impedance spectroscopic studies in TiO_2 -doped AgNbO_3 ceramic. *J. Alloys. Compounds* **2016**, 664, 715–725.
- (23) Wu, F. J.; Li, X.; Liu, W.; Zhang, S. T. Highly enhanced photocatalytic degradation of methylene blue over the indirect all-solid-state Z-scheme $\text{g-C}_3\text{N}_4\text{-RGO-TiO}_2$ nanoheterojunctions. *Appl. Surf. Sci.* **2017**, 405, 60–70.
- (24) Souza, F. L.; Lopes, K. P.; Nascente, P. A.; Leite, E. R. Nanostructured hematite thin films produced by spin-coating deposition solution: application in water splitting. *Sol. Energ. Mat. Sol. C* **2001**, 93, 362–368.
- (25) Lin, H. X.; Xu, Z. T.; Wang, X. X.; Long, J. J.; Su, W. Y.; Fu, X. Z.; Lin, Q. Photocatalytic and antibacterial properties of medical-grade PVC material coated with TiO_2 film. *J. Biomed. Mater. Res. A* **2008**, 87, 425–431.
- (26) Cadiam, M. B.; Rajangam, V.; Balachandran, S.; Aziz, A.; Hyun, T. J. Characterization of reduced graphene oxide supported mesoporous $\text{Fe}_2\text{O}_3/\text{TiO}_2$ nano-particles and adsorption of As(III) and As(V) from potable water. *J. Taiwan. Inst. Chem. E* **2016**, 62, 199–208.
- (27) Hua, A.; Pan, D. H.; Yong, L.; Luan, J.; Wang, Y.; He, J. Fe_3Si -core/amorphous-C-shell nanocapsules with enhanced microwave absorption. *J. Magn. Mater.* **2019**, 471, 561–567.
- (28) Zhang, C.; Wu, Q.; Ke, X. Elaboration and characterization of nanoplate structured $\alpha\text{-Fe}_2\text{O}_3$ films by Ag_3PO_4 . *Sol. Energy* **2016**, 135, 274–283.
- (29) Han, H.; Riboni, F.; Karlicky, F. $\alpha\text{-Fe}_2\text{O}_3/\text{TiO}_2$ 3D hierarchical nanostructures for enhanced photoelectrochemical water splitting. *Nanoscale* **2016**, 9, 134–142.
- (30) Liu, G. L.; Zhu, D. W.; Liao, S. J.; Ren, L. Y.; Cui, J. Z.; Zhou, W. B. Solid-phase photocatalytic degradation of polyethylene-goethite composite film under UV-light irradiation. *J. Hazard. Mater.* **2009**, 172, 1424–1429.
- (31) Deng, W. H.; Ning, S. B.; Lin, Q. Y.; Zhang, H. L.; Zhou, T. H. I- TiO_2/PVC film with highly photocatalytic antibacterial activity under visible light. *Colloids. Surf. B* **2016**, 144, 196–202.
- (32) Yan, X.; Xue, C.; Yang, B.; Yang, G. Novel three-dimensionally ordered macroporous Fe^{3+} -doped TiO_2 photocatalysts for H_2 production and degradation applications. *Appl. Surf. Sci.* **2017**, 394, 248–257.
- (33) Ng, T. W.; Zhang, L. S.; Liu, J. S.; Huang, G. C.; Wang, W.; Wong, P. K. Visible-light-driven photocatalytic inactivation of Escherichia coli by magnetic $\text{Fe}_2\text{O}_3\text{-AgBr}$. *Water. Res.* **2016**, 90, 111–118.
- (34) Kim, S. H.; Kwak, S. Y.; Suzuki, T. Photocatalytic degradation of flexible PVC- TiO_2 nanohybrid as an eco-friendly alternative to the current waste landfill and dioxine-emitting incineration of post-use PVC. *Polymer* **2006**, 47, 3005–3116.
- (35) Cho, S. M.; Choi, W. Y. Solid-phase photocatalytic degradation of PVC- TiO_2 polymer composites. *J. Photoch. Photobio. A* **2001**, 143, 221–228.
- (36) Xie, J.; Zhou, Z.; Lian, Y.; Hao, Y.; Li, P.; Wei, Y. Synthesis of $\alpha\text{-Fe}_2\text{O}_3/\text{ZnO}$ composites for photocatalytic degradation of pentachlorophenol under UV-vis light irradiation. *Ceram. Int.* **2015**, 41, 2622–2625.
- (37) Moumeni, O.; Hamdaoui, O. Intensification of sonochemical degradation of malachitegreen by bromide ions. *Ultrason. Sonochem.* **2012**, 19, 404–409.